Journal of Neurochemistry

JOURNAL OF NEUROCHEMISTRY | 2008 | 106 | 2312–2321 doi: 10.1111/j.1471-4159.2008.05557.x

Identification and characterization of a novel, shorter isoform of the small conductance Ca^{2+}-activated K^+ channel SK2

Saravana R. K. Murthy,* Georgeta Teodorescu,† Ingrid M. Nijholt,‡ Amalia M. Dolga,‡ Stephan Grissmer,† Joachim Spiess*,§ and Thomas Blank*,§

*Molecular Neuroendocrinology Laboratory, Max Planck Institute for Experimental Medicine, John A. Burns School of Medicine, University of Hawaii, Honolulu, Hawaii, USA

†Department of Applied Physiology, University of Ulm, Ulm, Germany

‡Department of Molecular Neurobiology, University of Groningen, Haren, The Netherlands

§Specialized Neuroscience Research Program 2, John A. Burns School of Medicine, University of Hawaii, Honolulu, Hawaii, USA

Abstract

Throughout the CNS, small conductance Ca^{2+}-activated potassium (SK) channels modulate firing frequency and neuronal excitability. We have identified a novel, shorter isoform of standard SK2 (SK2-std) in mouse brain which we named SK2-sh. SK2-sh is alternatively spliced at exon 3 and therefore lacks 140 amino acids, which include transmembrane domains S3, S4 and S5, compared with SK2-std. Western blot analysis of mouse hippocampal tissue revealed a 47 kDa protein product as predicted for SK2-sh along with a 64 kDa band representing the standard SK2 isoform. Electrophysiological recordings from transiently expressed SK2-sh revealed no functional channel activity or interaction with SK2-std. With the help of real-time PCR, we found significantly higher expression levels of SK2-sh mRNA in cortical tissue from AD cases when compared with age-matched controls. A similar increase in SK2-sh expression was induced in cortical neurons from mice by cytokine exposure. Substantial clinical evidence suggests that excess cytokines are centrally involved in the pathogenesis of Alzheimer's disease. Thus, SK2-sh as a downstream target of cytokines, provide a promising target for additional investigation regarding potential therapeutic intervention.

Keywords: Alzheimer's disease, cortical neurons, small conductance calcium-activated potassium channel, splice variant, whole-cell recordings.

J. Neurochem. (2008) **106**, 2312–2321.

Three SK channel subunits have been cloned (SK1-3), which exhibit distinct but partly overlapping distributions in the central nervous system (Kohler *et al.* 1996; Bond *et al.* 1999). The three subunits are highly homologous and have indistinguishable biophysical properties in terms of single channel conductance, rectification, selectivity and gating, which is governed by Ca^{2+} -binding to calmodulin constitutively attached to the C-terminus of each subunit. *In situ* hybridization (Stocker and Pedarzani 2000) and immunohistochemistry revealed a close correlation between apamin-sensitive currents, which are believed to underlie medium afterhyperpolarizations (mAHPs) and the distribution of apamin-sensitive SK2 channels in the adult rat hippocampus (Sailer *et al.* 2002). Indeed, transgenic mice lacking SK2 channel genes completely lack the apamin-sensitive component of the current ascribed to the mAHP in hippocampal CA1 neurons (Bond *et al.* 2004). In line with these findings are apparent reductions in mAHP amplitude and increased excitability after apamin application in CA1 pyramidal cells (Stocker *et al.* 1999; Stackman *et al.* 2002). In contrast to these reports, Gu *et al.* (2005) found that blockade of SK2 channels by apamin failed to affect the mAHP of rat CA1 pyramidal cells. The contribution of SK2 to the control of neuronal excitability apparently differs between brain areas

Received March 5, 2008; revised manuscript received June 5, 2008; accepted June 27, 2008.

Address correspondence and reprint requests to: Thomas Blank, Ph.D., University of Hawaii, John A. Burns School of Medicine, SNRP2, 651 Ilalo Str., Honolulu, HI 96813, USA.
E-mail: tblank@hawaii.edu

Abbreviations used: AHP, afterhyperpolarization; AP, alkaline phosphatase; EST, expressed sequence tag; GR, glucocorticoid receptor; GRE, glucocorticoid response element; HEK293 cells, human embryonic kidney 293 cells; MR, mineralocorticoid receptor; PBS, phosphate-buffered saline; PCR, polymerase chain reaction; SK, small conductance Ca^{2+}-activated potassium channel; TNF-α, tumor necrosis factor-α.

in view of the finding that over-expression of SK2 in mice enhanced the mAHP in neocortical pyramidal cells (Villalobos *et al.* 2004). Recent biochemical experiments have revealed that SK2 channels can reside within a complex multiprotein assembly comprising at least a kinase (CK2) and a phosphatase (PP2) (Bildl *et al.* 2004; Allen *et al.* 2007). Ca^{2+} sensitivity of SK2 channels is regulated in a dynamic manner, directly through CK2 and PP2A, and indirectly by Ca^{2+} itself via the state dependence of CaM phosphorylation by CK2 (Allen *et al.* 2007). Besides the initially reported SK2 standard form (SK2-std), a second SK2 isoform (SK2-L) with an N-terminal extension has been described (Strassmaier *et al.* 2005). The extended sequence unique to SK2-L contains an SH3-binding site as well as a potential mitogen-activated protein kinase substrate and several serine and threonine residues that may also serve as targets for phosphorylation. It was shown that SK2-L is expressed in a subset of SK2-expressing neurons and co-assembles with the other SK subunits.

The reported SK2 channel isoforms have a marked homology within their typical six transmembrane domain topology and distribution in the brain. In the present study, we characterized a novel, shorter SK2 isoform (SK2-sh), which is lacking transmembrane domains S3, S4 and S5 and which shows a distinct expression pattern in the mouse brain when compared with all other reported SK channel subtypes. In cortical cell culture, the expression of SK2-sh protein was elevated in the presence of the cytokine tumor necrosis factor-α alone or in combination with glutamate. Because tumor necrosis factor-α is over-expressed in AD brains (Vesce *et al.* 2007), we investigated possible alterations of SK2-sh expression in postmortem human cortical tissue from AD cases. Reverse transcription-PCR (RT-PCR) demonstrated a significantly higher abundance of SK2-sh mRNA in RNA isolated from aged controls and aged AD cases in comparison to young controls. The current findings expand our insights into the function of SK channels beyond their classical role as modulators of neuronal excitability and suggest a role in AD-associated defects.

Materials and methods

Rapid amplification of cDNA ends and cloning

To determine the full-length nucleotide sequence of mSK2sh mRNA, cDNA was amplified by RT-PCR and 5′and 3′ rapid amplification of cDNA ends (RACE) using a GeneRacer kit (Invitrogen, Carlsbad, CA, USA) according to the manufacturer's instructions. Gene-Racer-oligo(dT) primer, GeneRacer 3′ primer, and GeneRacer 5′ primer were provided with the kit, gene-specific primers SK2shAS1 primer (5′-CTGCACCCATGATTCCAGTA-3′) and SK2shAS2 primer (5′-TACTGGAATCATGGGTGCAG-3′) were designed for mSK2sh. Total RNA was isolated from C57BL/6J mouse hippocampal tissue, using the total RNA isolation system (Promega, Madison, WI, USA). The first-strand cDNA was synthesized using Superscript II RT with the GeneRacer oligo(dT) primer at 42°C for 1 h. 3′ RACE PCR was performed with the GeneRacer 3′ primer and a gene-specific primer (AS1) under the following conditions: one cycle of 94°C for 2 min, five cycles of 94°C for 30 s and 72°C for 1 min, five cycles of 94°C for 30 s and 70°C for 1 min, 30 cycles of 94°C for 30 s, 55°C for 30 s, 68°C for 2 min and one cycle of 68°C for 10 min. To obtain the 5′-end, the dephosphorylated and decapped mRNA was ligated with Gene Racer RNA oligonucleotides and the first-strand cDNA was reverse-transcribed using Thermoscript RT (Invitrogen) with AS2 as a primer at 65°C for 60 min. 5′ RACE PCR was performed with the GeneRacer 5′ primer and AS2 under the following conditions: one cycle of 94°C for 2 min, five cycles of 94°C for 30 s and 72°C for 1 min, five cycles of 94°C for 30 s and 70°C for 1 min, 30 cycles of 94°C for 30 s, 55°C for 30 s, 68°C for 1 min and one cycle of 68°C for 10 min. 5′ and 3′ RACE PCR products were used to produce the full-length SK2-sh cDNA by splice overlap PCR.

RNA preparation and cDNA synthesis

Total RNA from individual tissue samples was isolated using sv total RNA isolation system (Promega). cDNA was synthesized from 1 μg of total RNA with Transcriptor First Strand cDNA Synthesis Kit (Roche Applied Science, Indianapolis, IN, USA), using random hexamers as primers according to the manufacturer's instructions. RNA and DNA concentration and yield was determined by optical density (OD) measurements at 260 and 280 nm using a GeneQuant *pro* spectrophotometer (Amersham, Cambridge, UK).

Reverse transcriptase PCR

Primers were designed at the exon junctions of SK2-sh and SK2-std transcripts for human, mouse and rat (listed in Table 1). RT-PCR was performed with 0.5 μg total RNA, 5 pmol primers using OneStep RT-PCR Kit (Invitrogen, Karlsruhe, Germany) The thermal cycling conditions were 55°C for 30 min, 95°C for 15 min, 35 cycles of 95°C for 30 s, 60°C for 30 s and 72°C for 10 s. The amplified products were monitored by electrophoresis in a 2% agarose gel with Tris-acetate EDTA buffer. A negative control was included for every reaction without the RNA. To analyze the amplicons, the amplified products were cloned into the pCR2.1-TOPO vector (Invitrogen). Subcloned fragments were reamplified using the same primers and the insert was confirmed by sequencing.

Quantitative real-time PCR

The cDNA was analyzed in quantitative real-time PCR on a Roche Lightcycler 2 (Roche Applied science). All primers were designed

Table 1 Primer sequences

Target	Primer name	Sequence
Human SK2-sh	hSK2shFwd	5′-GGGAAATACAGTACCATGATC-3′
Human SK2-sh	hSK2shRev	5′-TATCAACCACATCGCTCCAA-3′
Mouse SK2-sh	mSK2shFwd	5′-GGGAAATACAGTACCATGATC-3′
Mouse SK2-sh	mSK2shRev	5′-CTGCACCCATGATTCCAGTA-3′
Rat SK2-sh	rSK2stdFwd	5′-GGGAAATACAGTACCATGATC-3′
Rat SK2-sh	rSK2stdRev	5′-CTGCACCCATGATTCCAGTA-3′

with Roche Probe Design 2 software (Roche Applied science; Table 1). Each real-time PCR reaction was prepared with a total volume of 20 μL containing 1 μL cDNA, 0.25 μmol/L of each primer and 4 μL of LightCycler FastStart DNA Master-PLUS SYBR Green I master mix (Roche Applied science). The following conditions were utilized for real-time PCR: initial denaturation for 3 min at 95°C, followed by 45 cycles of 15 s at 95°C, 15 s at 60°C and 5 s at 72°C. This was followed by one cycle of melting and subsequent cooling to 15°C. All real-time PCR experiments were performed in duplicate and repeated twice. A negative control for each primer pair and a positive control with 25 ng of mouse genomic DNA were included in each tube. The sensitivity of reactions and amplification of contaminant products was evaluated by amplifying serial dilutions of cDNA (1, 1 : 10, 1 : 100, 1 : 1000) and one sample containing reaction mixture without cDNA. To obtain absolute quantification, standard curves were plotted for every assay and were generated using defined concentrations of SK2-sh, and SK2-std cDNA cloned in pcDNA3.1. Standard curves for each amplicon were plotted from eight different concentrations of standards, each run in triplicate. Concentrations were determined by spectrophotometry and purity confirmed by agarose gel electrophoresis. The threshold cycle, Ct, which correlates inversely with the target mRNA levels, was measured as the cycle number at which the reporter fluorescent emission increased above a pre-set threshold level.

In situ hybridization of mouse SK2-sh mRNA

Six brains from C57BL/6J mice were removed and frozen in liquid nitrogen. Coronal sections (20 μm thick) were prepared with a microtome, thaw-mounted onto SuperFrost Plus slides (Fischer, Pittsburgh, PA), fixed in 4% paraformaldehyde, followed by washing in phosphate-buffered saline (PBS) and dehydration in graded series of ethanol. Oligonucleotide probes complementary to mouse SK2-sh mRNA antisense strand (5′-GTGACATCCTGTTGATCATGG-TACTGTATTTCCCTGGCGTGGTACACGAA-3′) and SK2-sh sense (5′-ATCGTGTACCACGCCAGGGAAATACAGTACCATG-ATCAACAGGATGTCAC-3′) were end-labeled with 33P at 37°C for 10 min using a terminal deoxynucleotidyl transferase kit (Roche, Mannheim, Germany). The sections were incubated overnight in hybridization buffer (50% formamide, 10% dextran sulfate, 50 mM dithiothreitol, 0.3M NaCl, 30 mM Tris–HCl (pH 7.4), 4 mM EDTA (pH 8), IX Denhardts solution, 0.5 mg/mL salmon sperm DNA and 0.5 mg/mL Poly A DNA) at 48.6°C. Post-hybridization washes were carried out in 1× standard sodium citrate (SSC) (150 mM NaCl, 30 mM Na citrate, pH 7.2) for 2 × 2 min at 21°C, followed by a stringent wash at 57°C in 1× SSC for 45 min. The slides were subsequently washed in progressively diluted SSC buffers and then dehydrated in aqueous ethanol (50–100%). After dehydration in an ascending ethanol series, the sections were air dried at 21°C and dipped in NBT-2 emulsion (Kodak) diluted 1 : 1 with distilled water. After exposure for 1 month at 4°C, the dipped slides were developed in Kodak D-19 developer and fixed. Afterwards images were captured by darkfield microscopy (Axioplan-2, Carl Zeiss, Oberkochen, Germany). Digital images of each section were captured by a digital camera and analyzed with WinROOF analysis software (Mitani Co., Fukui, Japan). Before emulsion staining, slides were air-dried and exposed to Kodak Biomax MR-Roentgen film for 24–48 h.

Construction of SK2-sh His tagged expression vector and transient transfection of human embryonic kidney (HEK) 293 cells

The open reading frame of mSK2-sh was amplified from mSK2sh/pCR4-TOPO vector with primers mSK2shFwd (5′-ATGAGCA-GCTGCAGGTAC-3′) and mSK2shRev (5′-GCTACTCTCTGAT-GAAGTTGGT-3′). After the PCR fragment was gel extracted it was cloned into a pcDNA3.1His vector (Invitrogen) in frame with the polyHistidine repeats and confirmed by sequencing. HEK293 cells were maintained in Dulbecco's modified Eagle's medium (DMEM, Gibco, Rockville, MD, USA) containing 10% fetal calf serum (Gibco) and 2 mM glutamine in a 37°C humidified incubator with 5% CO_2 and split 1 : 10 twice weekly. HEK293 cells were plated in 6-well plates on poly-D-lysine-coated glass cover slips and once 40–50% confluence had been reached, cells were transiently transfected using FuGene 6 (Roche Molecular Biochemicals) with 6 μg mSK2sh DNA construct in serum-free OptiMEM medium (Life Technologies, Inc.). Cells were plated 24 h following transfection for overnight growth and subsequent labeling studies.

Identification of fluorescein isothiocyanate-labeled mSK2-sh in HEK293 cells

Cells were washed twice with cold PBS containing 10 mm $MgCl_2$, 0.1% (w v-1) D-glucose and 0.2% (w v-1) bovine serum albumin, fixed with 100% methanol and washed twice in PBS. Fetal bovine serum (10% in PBS) was applied to block non-specific binding. Subsequently, cells were exposed to anti-His (C-term)-FITC antibody (1 : 500 dilution) (Invitrogen) either alone or in the presence of excess cold, unlabeled anti-His(C-term) antibody. Cells were incubated for 1 h at 21°C in the dark. After incubation, cells were washed twice with PBS and identified under a fluorescent microscope (Carl Zeiss Inc., Thornwood, NY, USA) equipped with FITC filters. FITC images were collected using appropriate bandpass filters at an excitation wavelength of 488 nm and an emission wavelength of 520 nm. The images were analyzed by AXIO image software (Carl Zeiss Microimaging, Goettingen, Germany).

Whole-cell patch clamp experiments-transient transfection of tsA201 cells

tsA cells were plated in 35-well plates and once 50–70% confluence had been reached, cells were transiently transfected using FuGene 6 (Roche Molecular Biochemicals, Germany) with 3 μg mSK2sh DNA construct and 0.5 μg pEGFP vector (BD Bioscience Clontech, Palo Alto, CA, USA), in serum-free DMEM medium (Life Technologies, Inc.). Cells were plated 24 h following transfection for overnight growth and used for electrophysiological studies 48–72 h after transfection. Cells were superfused with N-sol, (in mM: NaCl 160, KCl 4.5, HEPES 5, $MgCl_2$ 1 and $CaCl_2$ 2) with pH 7.4 adjusted with NaOH. Pipettes were pulled in three stages with a pipette resistance ranging from 1.5 to 2.5 MΩ when filled with K-Asp solution containing 1 μM free Ca^{2+} (in mM: K^+ aspartate 135, K-EGTA 10, HEPES 10, $MgCl_2$ 2, $CaCl_2$ 8.422 corresponding to 1 μM of free Ca^{2+}, pH 7.2 adjusted with KOH). After whole-cell perfusion with K-Asp solution containing 1 μM free Ca^{2+}, the membrane potential was clamped to −120 mV for 50 ms followed by a 400-ms voltage ramp from −120 to +60 mV using a HEKA EPC9 amplifier with Pulse and PulseFit (HEKA elektronik, Germany) as data acquisition and analysis software. The membrane potential was kept at −80 mV for 5 s between ramps.

Primary cortical neuronal culture

Cortical neurons were prepared from embryonic brains (E15-16) of C57Bl/6J mice. The meninges were removed and the cortical neurons were separated by mechanical dissociation. Cells were plated in a density of 2×10^6 cells/well (6-well plates) on 2 μg/mL poly-D-lysine-coated plates. Neurobasal medium with B27-supplement (Invitrogen, Gibco BRL, Carlsbad, CA, USA), 0.5 mM glutamine, 1% penicillin/streptomycin and 2.5 μg/mL amphotericin B was used as a culture medium. After 48 h cells were treated with 10 μM cytosine arabinoside for another 2 days, to inhibit non-neuronal cell growth. Subsequently, the medium was completely exchanged and after 6 days of *in vitro* culture, the neurons were used for experiments. Cells were incubated over a period of 24 h with 100 ng/mL tumor necrosis factor-α (TNF) (kindly provided by HBT, Uden, The Netherlands). Excitotoxicity was induced by different concentrations of glutamate (100 μM) for 1–4 h. After treatment, the media was completely removed and the neurons were lysed for western blot analysis.

Western blots and protein analysis

Primary cortical neurons from C57Bl/6J mice were washed twice with ice-cold PBS and subsequently lysed by the addition of 0.15 mL lysis buffer (20 mM Tris, 150 mM NaCl, 1 mM EDTA, 1 mM EGTA, 1% Triton, 2.5 mM sodium pyrophosphate, 1 mM sodium orthovanadate and Complete mini protease inhibitor cocktail tablet (Roche). The samples were centrifuged at 9000 *g* for 10 min at 4ºC and the supernatants were boiled for 5 min in Laemmli's sample buffer (2% SDS, 5% dithiothreitol). Twenty micrograms of total protein was separated by 10% SDS-polyacrylamide gel electrophoresis. After transfer to a polyvinylidene fluoride transfer membrane (Millipore Corporation, Bedford, MA, USA) proteins were detected with a specific primary antibody and an alkaline phosphatase (AP)-labeled secondary antibody using the electrochemiluminescent detection system according to the manufacturer's instructions (Tropix). Primary antibodies used were a rabbit polyclonal antibody specific for SK2 (kindly provided by Hans-Günther Knaus, University of Innsbruck) (1 : 4000 dilution) and a monoclonal mouse antibody specific for actin (MP Biomedicals, Irvine, CA, USA) (1 : 100 000 dilution). The actin was taken as an internal control to correct for variations in protein content. The blots were incubated with AP-conjugated secondary antibodies: AP-conjugated goat anti-mouse (Tropix) (1 : 10 000 dilution) and AP conjugated goat anti-rabbit (Tropix) (1 : 10 000 dilution). Integrated optical densities were measured by the Leica DFC 320 Image Analysis System (Leica, Cambridge, UK) and densitometric analysis was evaluated by the Leica Qwin program (Leica). Integrated optical densities measurements were corrected for the background intensity.

Brain tissue samples

Human brain tissue from Alzheimer's disease (AD) cases (range 73–85 years, average 81 years), age-matched controls (range 73–91 years, average 85 years) and young controls (range 33–43 years, average 38 years) was kindly provided by Prof. Rob de Vos, Department of Neurology MST Hospital Group and Pathology Lab Oost Nederland. All three groups contained approximately the same amount of males and females. The histopathological diagnosis of AD was performed according to the CERAD (Consortium to Establish a Registry for Alzheimer's Disease, Mirra *et al.* 1991, 1993) criteria, and for each case, the neuropathological Braak staging was determined (Braak and Braak 1991). Braak stages I and II with mild to moderate alterations within the transentorhinal region correspond to the preclinical stage of AD and were classified as controls. Cases corresponding to Braak stages III–VI were included in the AD group. Tissue blocks were collected from the entorhinal cortex at autopsy (postmortem time 20–46 h) based on written informed consent for use of the obtained brain tissue for research. All brain tissue was flash frozen in liquid nitrogen and stored at −80°C until use.

Statistics

Statistical comparisons were made using Student's *t*-test or ANOVA. All RT-PCR experiments were repeated at least twice. Data are expressed as mean ± standard error (SEM). The significance was determined at the level of $p < 0.05$.

Results

Identification, cloning and protein sequence of SK2-sh, a novel SK2 splice variant

The primary identification of the expressed sequence tag (EST) encoding SK2-sh as a novel SK2 (SK2-std) variant was performed by a basic local alignment search tool (BLAST) search of GenBank™ with the SK2 sequence (DR003610) from human hippocampus. SK2-std cDNA and EST sequences were further analyzed to confirm the exact difference in the alignment using the bl2seq tool (Tatusova and Madden 1999). A genomic BLAST of the selected EST was performed against the human genomic database with $E < 0.01$ and low complexity as parameters to find the distribution of the exons on the SK2 locus. The EST (DR003610) alignment on the human genome stretched from exon 1 to exon 6, skipping the third exon of 320 nucleotides in length of the SK2 gene. To determine whether this splice variant was also present in mouse and rat, an EST search was

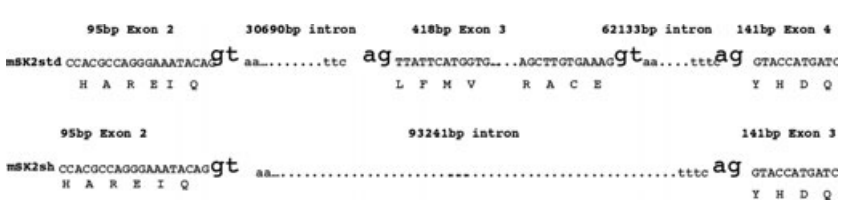

Fig. 1 Exon–intron junction and splice consensus sequence of SK2-std and SK2-sh. A portion of the SK2 gene locus is shown from exon 2 to exon 4 (exons not to scale). Splicing of exon 3 in SK2-sh leads to an 93.24 kb intron.

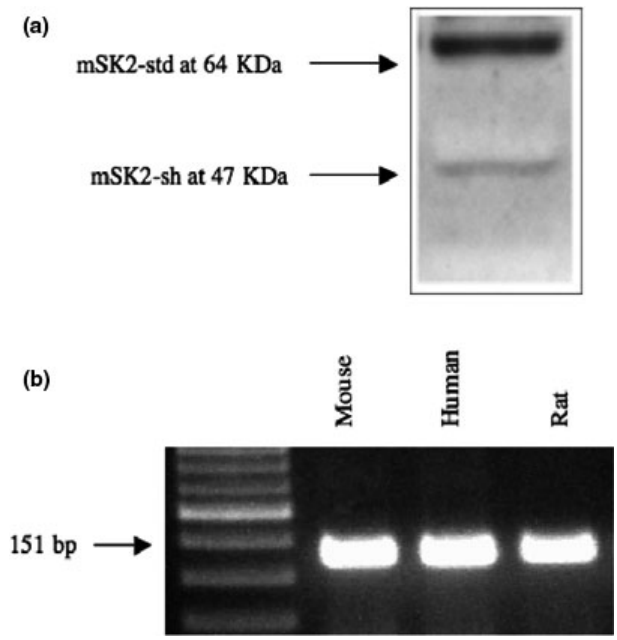

Fig. 2 Detection of SK2-sh in hippocampal tissue using western blot analysis and RT-PCR. (a) 64 and 47 KDa bands of mSK2-std and mSK2-sh, respectively, were detected in western blots from mouse hippocampal tissue using an antibody against the C-terminal region of mouse SK2. (b) SK2-sh was amplified from mouse, human and rat hippocampal RNA samples.

performed on the EST databases of mouse and rat, taking human EST as query. However, no comparable EST was found. Comparative genomic search at the spliced region of the EST (DR003610) in human, mouse and rat showed 100% conservation in all three organisms. The splice consensus sequence was also conserved across these species (Fig. 1).

Western blots with proteins isolated from mouse hippocampal tissue revealed a 64 and a 47 KDa band (Fig. 2a). They corresponded to the mouse SK2-std and mouse SK2-sh isoform, respectively. In order to determine the expression of the SK2-sh variant in human, mouse and rat hippocampus by RT-PCR, primers were designed for the specific splice exon junctions and amplified bands of 151 bp (Fig. 2b). PCR fragments were eluted and confirmed by sequencing. However, the copy number of this new variant was lower when compared to the copy number of SK2-std in all three species. To determine the full-length nucleotide sequence of mSK2sh mRNA, cDNA was amplified by RT-PCR and 5′and 3′ rapid amplification of cDNA ends (RACE). The full-length sequence of SK2-sh (EU478850 [GenBank]) was used to predict the protein sequence. Multiple alignments of mSK2-std and mSK2-sh protein sequences revealed that 140 amino acids were spliced out (exon 3). Splicing of exon 3 in SK2-sh resulted in omission of the three transmembrane domains S3, S4, and S5, whereas the pore-forming region, calmodulin binding domain (CamBD) and coiled coil regions were retained as in SK2-std (Fig. 3a and b).

Regional SK2-sh and SK2-std mRNA expression profile in mouse CNS and peripheral tissue

To address the tissue distribution of SK2-sh and SK2-std mRNA across different mouse tissues, we developed variant-specific quantitative RT-PCR. SK2-sh was abundantly expressed in olfactory lobes and heart tissue. Low expression levels were found in the hippocampus, cortex, cerebellum, retina, lung, liver and skeletal muscle (Fig. 4a). Under baseline conditions, the expression level of SK2-sh was much lower than the expression level of SK2-std (Fig. 4b). SK2-std was also expressed in tissues where SK2-sh could not be detected, such as trachea, kidney, stomach, testis, bone

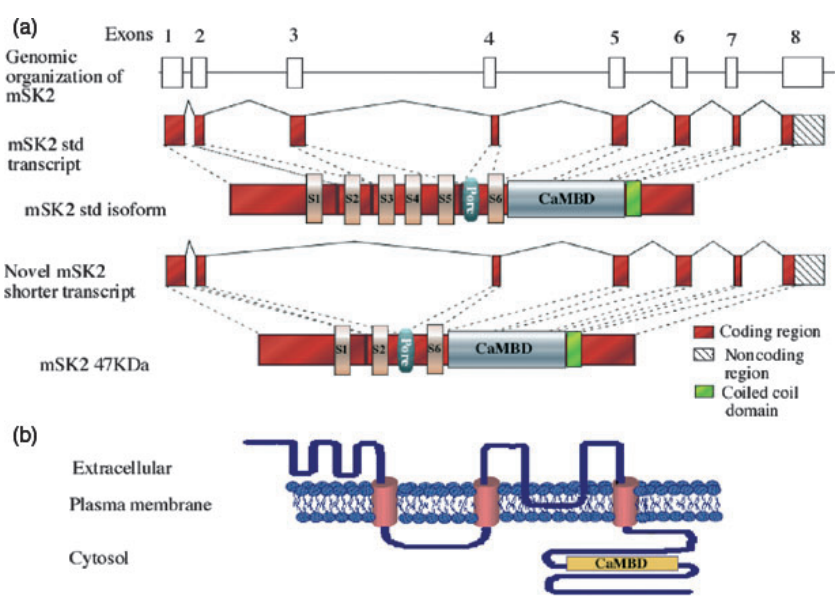

Fig. 3 Genomic organization, splice junction and topology of SK2-std and SK2-sh. (a) Diagrammatic representation of exon–intron positions on the mouse genomic SK2 locus, mRNA transcripts of SK2-std and SK2-sh. Exons are numbered 1–8 (not to scale) and represented as boxes on the genome, which is represented as line. (b) Predicted membrane topology of SK2sh.

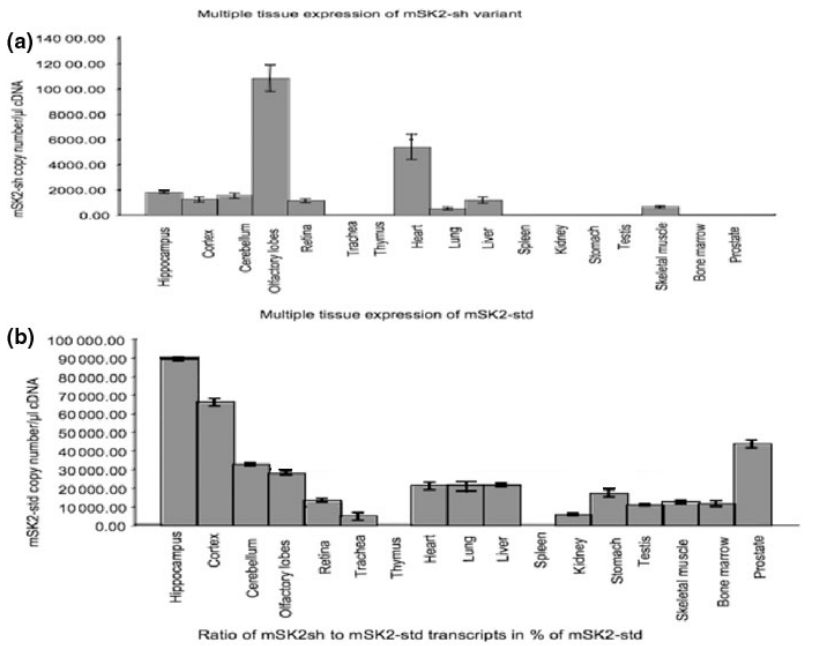

Fig. 4 Distribution of mSK2-std and mSK2-sh in different mouse tissues determined by DNA Master-PLUS SYBR Green quantitative RT-PCR. mRNA copy numbers are shown per microlitre of cDNA from various mouse tissues for (a) mSK2-sh and (b) mSK2-std. (c) The ratio between mSK2-sh and mSK2-std is presented in percentage. Data are expressed as means ± SE, n = 3–9 per group.

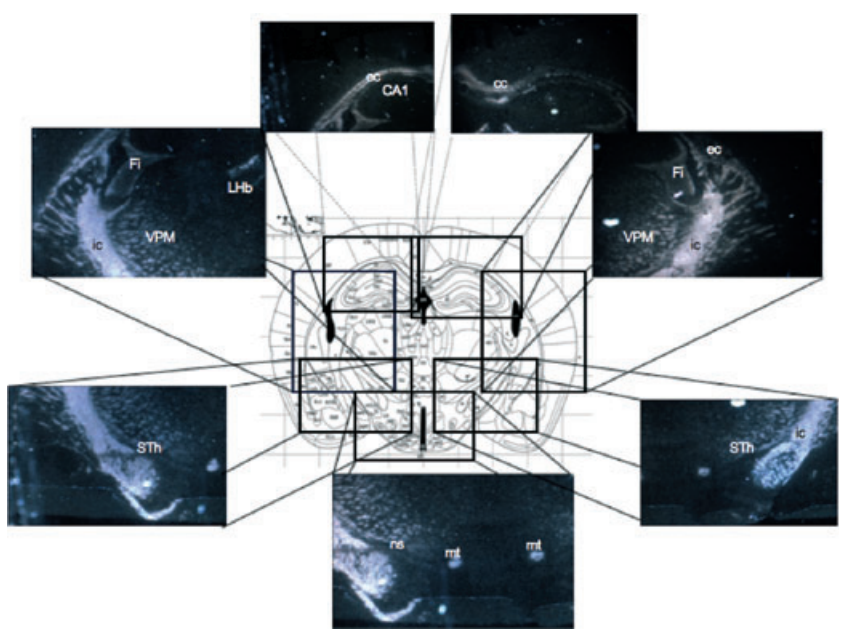

Fig. 5 Distribution of SK2-sh in mouse brain. *In situ* hybridization and emulsion staining of coronal section as (a), overview after Franklin and Paxinos (1997) or (b) divided into regional subfields. Positive hybridization signals for SK2-sh mRNA were found in *fi*, fimbria of the hippocampus; *st*, stria terminalis; *cg*, cingulum; *cc*, corpus callosum; *ec*, external capsule; *LHbL*, lateral habenular nucleus lateral part; *LHbM*, lateral habenular nucleus, medial part; *mt*, mammillothalamic tract; *STh*, subthalamic nucleus; *MCLH*, magnocellular nucleus of the lateral hypothalamus; *ic*, internal capsule.

marrow and prostate (Fig. 4b). Comparison of SK2-sh splice variant mRNA expression to SK2-std mRNA expression across tissues demonstrated a certain degree of tissue heterogeneity only in olfactory lobes and heart (Fig. 4c). In all other investigated tissues, SK2-sh was expressed at <10% of SK2-std mRNA.

SK2-sh localization in mouse brain

Using *in situ* hybridization, we characterized the mRNA expression pattern of SK2-sh in the adult mouse brain (Fig. 5a and b). SK2-sh hybridization signals were present in distinct brain areas, which differed largely from the areas with positive SK2-std hybridization signals in rats (Kohler *et al.* 1996) and SK2-std protein levels in mice (Sailer *et al.* 2004). Of special note was the low SK2-sh hybridization level in cortex and hippocampus where SK2 channel function contributes significantly to regulation of neuronal excitability (Stocker *et al.* 1999). SK2-sh mRNA was found in the fimbria (fi), which is a main output pathway of the hippocampus and in the corpus callosum (cc).

Expression of SK2-sh in HEK293 cells and functional properties

To elucidate the cellular localization of SK2-sh, SK2-sh cDNA was subcloned into a mammalian expression vector, pcDNA3.1/His. After transient transfection, HEK293 cells expressed His-tagged SK2-sh protein, which was localized, using an anti-HIS tag antibody, in or close to the plasma membrane and showed only scattered distribution in the cytosol (Fig. 6a). Anti-HIS tag antibodies gave no positive signal after transfection of HEK293 cells with the pcDNA3.1/His vector alone (data not shown). To address whether SK2-sh can form functional channels, whole-cell recordings were performed from tsA cells expressing SK2-sh and SK2-std separately or in combination. Currents in response to a voltage ramp from −120 to +60 mV were as expected for SK2-std (Fig. 6b). However, SK2-sh showed no detectable current over the indicated membrane potential range and had no significant effect on SK2-std currents when co-expressed. Similarly, the SK2-std maximum whole-cell conductance was not significantly affected by co-expression of SK2-sh (Fig. 6c).

SK2-sh mRNA in cortical tissue from AD cases

In order to determine a potential physiological significance of SK2-sh for brain function, we compared the expression pattern with known mRNA expression pattern under pathological conditions. We found that the expression pattern of SK2-sh in mouse brain was identical to that of apolipoprotein D (ApoD), which is thought to be involved in the neuropathology of AD (Drayna *et al.* 1986; Boyles *et al.* 1990; Thomas *et al.* 2001). Thus, the expression level of SK2-sh was investigated in cortical tissue samples from AD cases (Fig. 7). A total of 14 human cortical tissue samples were analyzed, in which three samples were from young controls (ages ranging from 33 to 40 years), five samples were from aged controls (ranging from 73 to 91 years) and six samples were from AD cases, (ranging from 73 to 84 years). Interestingly, SK2-sh mRNA expression was significantly increased in AD samples when compared with age-matched and young controls.

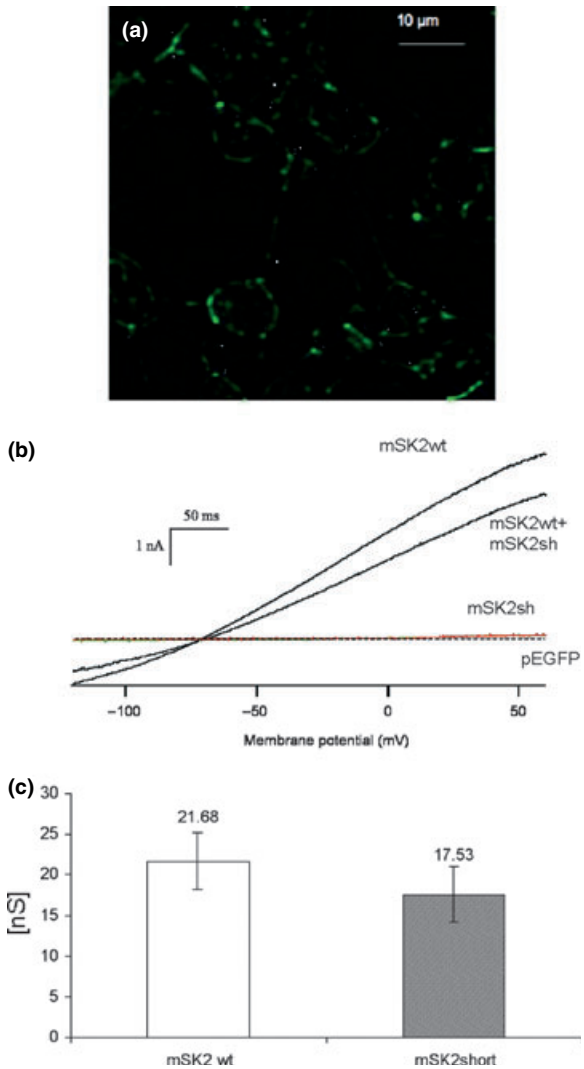

Fig. 6 Expression of His-tagged SK2-sh in HEK293 cells and electrophysiological recordings. (a) Anti-His antibody coupled to fluorescein was used to determine the cellular localization of the SK2-sh/His-tagged construct in HEK293 cells by fluorescence microscopy. SK2-sh was predominantly found integrated or in close proximity to the cell membrane. Only minor signals were detected inside the cytosol. (b) Whole-cell recordings from tsA201 cells transiently transfected with pEGFP, SK2-std and SK2-sh alone or in combination. Currents are shown in response to voltage ramp commands from −120 to +60 mV membrane potential (n = 10 cells). (c) Maximum conductance from whole-cell recordings of SK2-std and SK2-std co-expressed with SK2-sh in tsA201 cells (n = 9-10 cells).

Modulation of SK2-sh protein by TNF-α and glutamate

Alterations of astrocytic glutamate release by stimulation of TNF-α-dependent pathways can take place in the context of Alzheimer's disease (Rossi *et al.* 2005). TNF-α is a pro-inflammatory cytokine. Its two receptors are expressed on neurones and glial cells throughout the CNS. Through the

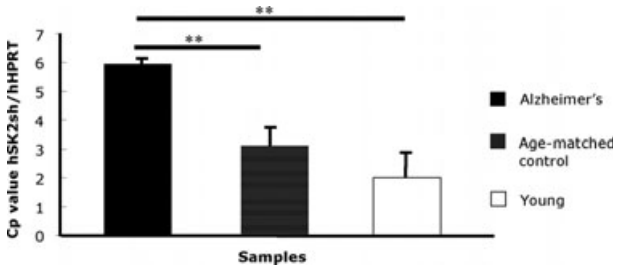

Fig. 7 Real-time PCR analysis of hSK2-sh mRNA expression in cortical tissue from AD cases. Increased expression of hSK2-sh mRNA in cortical tissue from AD cases compared with age-matched controls and young control subjects. mRNA samples from cortical tissues were used to generate cDNA and real-time PCR was performed to quantify mRNA levels. Samples from AD cases showed a substantial increase in hSK2-sh levels when compared with age-matched controls and young samples (**$p < 0.003$ and **$p < 0.0001$, respectively; $n = 5$). Standard deviations are shown as barlines. Statistics were done using ANOVA and Student's *t*-test.

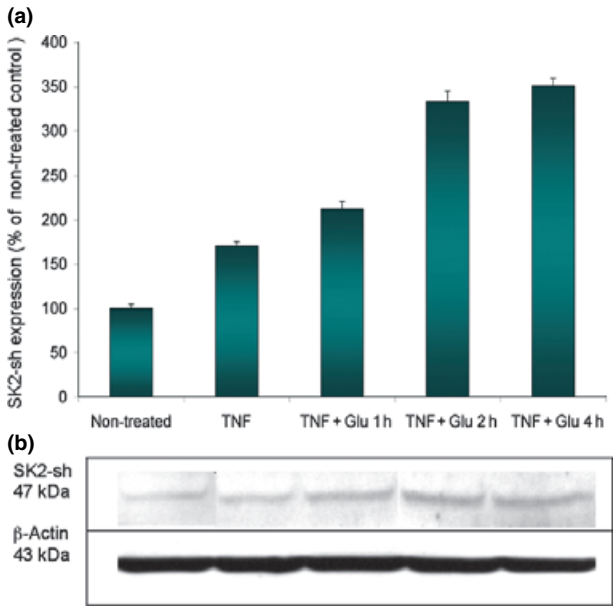

Fig. 8 Increased expression of SK2-sh after TNF-α and glutamate treatment in cortical neurons. (a) Bar graphs represent the optical density values for SK2-sh as percentage of non-treated neurons (set to 100%) obtained from western blot experiments using non-treated primary cortical neurons or primary cortical neurons treated with TNF-α (100 ng/mL, for 24 h) alone or together with glutamate (100 μM, for 1, 2 or 4 h) at the end of the TNF-α treatment. All of the bars depict the mean ± SE of three independent experiments, and the distribution of the data sets was analyzed by one-way ANOVA. (b) Representative western blot for SK2-sh after treatment of cortical neurons as indicated under (a). *β*-Actin was used as a loading control for western blot analysis.

action of its receptors, it has a broad range of actions on neurones which may be either neuroprotective or neurotoxic (Viviani *et al.* 2007). In order to determine the effect of TNF-α on SK2-sh protein levels, we exposed cortical neurons to 100 ng/mL TNF-α for the duration of 24 h and found increased level of SK2-sh protein by more than 60% when compared with the SK2-sh level in non-treated cortical neurons (Fig. 8a and b). In cortical neurons, which were incubated with 100 ng/mL TNF-α and challenged with additional 100 μM glutamate for the last 1, 2 and 4 h of the TNF-α treatment, SK2-sh protein levels showed a gradual increase following the duration of glutamate exposure (Fig. 8a and b). Glutamate alone did not change the expression of SK2-sh (data not shown).

Discussion

The evolution of alternative splicing mechanisms that target SK channel genes has served to amplify the structural diversity of these important proteins well beyond the basic pattern provided by three distinct gene classes (SK1-SK3). Characterizing the individual structural and functional properties that result from these splicing events represents an important challenge for the field. With this study we characterized SK2-sh as a novel SK2 variant, which has three transmembrane domains spliced out (140 amino acid) and appears to be a non-channel forming subunit. This is similar to SK3-1C and SK3-1B, variants of SK3, which do not produce functional channels when expressed alone in mammalian cells. However, SK3-1B selectively suppresses endogenous SK3 currents in the pheochromocytoma cell line, PC12 (Tomita *et al.* 2003) and SK3-1C suppresses SK1, SK2 and SK3 channel function (Kolski-Andreaco *et al.* 2004). In contrast, the co-expression of SK2-sh together with SK2-std had no effect on the currents generated by SK2-std. This might not seem surprising since SK2-std and SK2-sh do not show overlapping expression pattern in brain sections from naïve mice. SK2 expression has been described previously in mouse and rat brains (Stocker and Pedarzani 2000; Sailer *et al.* 2004), where it was concluded that SK2 channels are exclusively expressed in gray matter structures of the brain. The SK2-sh tissue distribution suggests that the regulation of SK2-sh at the promoter level must be different from that of SK2-std. We have previously identified one functional glucocorticoid response element at position −2248 bp and two functional nuclear factor-kappB (NF-kappaB) response elements at positions −1652 and −1586 bp in the SK2-std promoter (Kye *et al.* 2007). It can be speculated that transcription of the SK2 gene can be initiated from additional, independent genomic regions. The findings, so far, imply that tissue-specific expression of the SK2 gene is controlled by multiple alternative promoters. Both, alternative promoter usage and alternative splicing contribute to the remarkable mRNA diversity of the gene. Interestingly, the expression of SK2-sh in cortical neurons

increases in the presence of TNF-α. TNF-α is widely expressed in microglia and astrocytes and for many years these cells were believed to be the primary sources of this cytokine in the CNS (Kolski-Andreaco *et al.* 2004). However, different neuronal cell types may also produce TNF-α, particularly under pathological conditions (Liu *et al.* 1994; Knoblach *et al.* 1999). Several studies have shown that TNF-α exerts neuroprotective properties against glutamate-induced excitotoxicity in cortical neurons (Cheng *et al.* 1994; Marchetti *et al.* 2004). From this point of view it might be concluded that SK2-sh is involved in non-gating functions that are cell type-specific. One of these functions may be neuroprotection and might explain the additional increase in SK2-sh expression when cells were treated with TNF-α and glutamate. Increased levels of TNF-α in brain tissue, cerebrospinal fluid and plasma have been found in several CNS disorders, including Alzheimer's disease (Fillit *et al.* 1991). Here, the impact of TNF-α is supposed to elicit quite the opposite phenomenon, that is neurodegeneration through caspase-dependent cascades and silencing cell survival signals instead of neuroprotection (Takeuchi *et al.* 2006). We found that SK2-sh mRNA was over-expressed in brain tissue from AD cases. At present, we can only speculate whether under these pathological conditions SK2-sh is elevated to counteract detrimental effects of amyloid deposition or whether it is actively inducing massive neuronal cell death as a consequence of an uncontrolled inflammatory response. Our future experiments will be directed towards examining some of these specialized functions in more detail.

Acknowledgments

This work was supported by the Max-Planck Society.

References

Allen D., Fakler B., Maylie J. and Adelman J. P. (2007) Organization and regulation of small conductance Ca^{2+}-activated K^+ channel multiprotein complexes. *J. Neurosci.* **27**, 2369–2376.

Bildl W., Strassmaier T., Thurm H. *et al.* (2004) Protein kinase CK2 is coassembled with small conductance Ca^{2+}-activated K^+ channels and regulates channel gating. *Neuron* **43**, 847–858.

Bond C. T., Maylie J. and Adelman J. P. (1999) Small-conductance calcium-activated potassium channels. *Ann. NY Acad. Sci.* **868**, 370–378.

Bond C. T., Herson P. S., Strassmaier T., Hammond R., Stackman R., Maylie J. and Adelman J. P. (2004) Small conductance Ca2 +-activated K+ channel knock-out mice reveal the identity of calcium-dependent afterhyperpolarization currents. *J. Neurosci.* **24**, 5301–5306.

Boyles J. K., Notterpek L. M., Wardell M. R. and Ball S. C. J. (1990) Identifcation, characterization, and tissue distribution of apolipoprotein D in the rat. *J. Lipid Res.* **31**, 2243–2256.

Braak H. and Braak E. (1991) Neuropathological stageing of Alzheimer-related changes. *Acta Neuropathol. (Berl).* **82**, 239–259.

Cheng B., Christakos S. and Mattson M. P. (1994) Tumor necrosis factors protect neurons against excitotoxic insults and promote maintenance of calcium homeostasis. *Neuron* **12**, 139–153.

Drayna D., Fielding C., McLean J., Baer B., Castro G., Chen E., Comstock L., Henzel W., Kohr W. and Rhee L. (1986) Cloning and expression of human apolipoprotein D cDNA. *J. Biol. Chem.* **261**, 16535–16539.

Fillit H., Ding W., Buee L., Kalman J., Altstiel L., Lawlor B. and Wolf-Klein G. (1991) Elevated circulating tumor necrosis factor levels in Alzheimer's disease. *Neurosci. Lett.* **131**, 318–320.

Franklin K. B. J. and Paxinos G. (1997) *The mouse brain in stereotoxic coordinates*. San Diego, Academy Press.

Gu N., Vervaeke K., Hu H. and Storm J. F. (2005) Kv7/KCNQ/M and HCN/h, but not KCa2/SK channels, contribute to the somatic medium after-hyperpolarization and excitability control in CA1 hippocampal pyramidal cells. *J. Physiol.* **566**, 689–715.

Knoblach S. M., Fan L. and Faden A. I. (1999) Early neuronal production of Tumor necrosis factor-α after experimental brain injury contributes to neurological impairment. *J. Neuroimmunol.* **95**, 115–125.

Kohler M., Hirschberg B., Bond C. T., Kinzie J. M., Marrion N. V., Maylie J. and Adelman J. P. (1996) Small-conductance, calcium-activated potassium channels from mammalian brain. *Science* **273**, 1709–1714.

Kolski-Andreaco A., Tomita H., Shakkottai V. G., Gutman G. A., Cahalan M. D., Gargus J. J. and Chandy K. G. (2004) SK3-1C, a dominant-negative suppressor of SKCa and IKCa channels. *J. Biol. Chem.* **279**, 6893–6904.

Kye M. J., Spiess J. and Blank T. (2007) Transcriptional regulation of intronic calcium-activated potassium channel SK2 promoters by nuclear factor-kappa B and glucocorticoids. *Mol. Cell. Biochem.* **300**, 9–17.

Liu T., Clark R. K., McDonnell P. C., Young P. R., White R. F., Barone F. C. and Feuerstein G. Z. (1994) Tumor necrosis factor-alpha expression in ischemic neurons. *Stroke* **25**, 1481–1488.

Marchetti L., Klein M., Schlett K., Pfizenmaier K. and Eisel U. L. M. (2004) Tumor necrosis factor (TNF)-mediated neuroprotection against glutamate-induced excitotoxicity is enhanced by N-methyl-D-aspartate receptor activation. *J. Biol. Chem.* **289**, 32869–32881.

Mirra S. S., Heyman A., McKeel D., Sumi S. M., Crain B. J., Brownlee L. M., Vogel F. S., Hughes J. P., van Belle G. and Berg L. (1991) The Consortium to Establish a Registry for Alzheimer's Disease (CERAD). Part II. Standardization of the neuropathologic assessment of Alzheimer's disease. *Neurology* **41**, 479–486.

Mirra S. S., Hart M. N. and Terry R. D. (1993) Making the diagnosis of Alzheimer's disease. A primer for practicing pathologists. *Arch. Pathol. Lab. Med.* **117**, 132–144.

Rossi D., Brambilla L., Valori C. F. *et al.* (2005) Defective tumor necrosis factor-alpha-dependent control of astrocyte glutamate release in a transgenic mouse model of Alzheimer disease. *J. Biol. Chem.* **280**, 42088–42096.

Sailer C. A., Hu H., Kaufmann W. A., Trieb M., Schwarzer C., Storm J. F. and Knaus H. G. (2002) Regional differences in distribution and functional expression of small-conductance Ca^{2+}-activated K+ channels in rat brain. *J. Neurosci.* **22**, 9698–9707.

Sailer C. A., Kaufmann W. A., Marksteiner J. and Knaus H. G. (2004) Comparative immunohistochemical distribution of three small-conductance Ca^{2+}-activated potassium channel subunits, SK1, SK2, and SK3 in mouse brain. *Mol. Cell. Neurosci.* **26**, 458–469.

Stackman R. W., Hammond R. S., Linardatos E., Gerlach A., Maylie J., Adelman J. P. and Tzounopoulos T. (2002) Small conductance Ca^{2+}-activated K^+ channels modulate synaptic plasticity and memory encoding. *J. Neurosci.* **22**, 10163–10171.

Stocker M. and Pedarzani P. (2000) Differential distribution of three Ca(2 +)-activated K(+) channel subunits, SK1, SK2, and SK3, in the adult rat central nervous system. *Mol. Cell. Neurosci.* **15**, 476–493.

Stocker M., Krause M. and Pedarzani P. (1999) An apamin-sensitive Ca2 + -activated K+ current in hippocampal pyramidal neurons. *Proc. Natl Acad. Sci. USA* **96**, 4662–4667.

Strassmaier T., Bond C. T., Sailer C. A., Knaus H. G., Maylie J. and Adelman J. P. (2005) A novel isoform of SK2 assembles with other SK subunits in mouse brain. *J. Biol. Chem.* **280**, 21231–21236.

Takeuchi H., Jin S., Wang J., Zhang G., Kawanokuchi J., Kuno R., Sonobe Y., Mizuno T. and Suzumura A. (2006) Tumor necrosis factor-alpha induces neurotoxicity via glutamate release from hemichannels of activated microglia in an autocrine manner. *J. Biol. Chem.* **281**, 21362–21368.

Tatusova T. A. and Madden T. L. (1999) BLAST 2 Sequences, a new tool for comparing protein and nucleotide sequences. *FEMS Microbiol. Lett.* **174**, 247–250.

Thomas E. A., Sautkulis L. N., Criado J. R., Games D. and Sutcliffe J. G. (2001) Apolipoprotein D mRNA expression is elevated in PDAPP transgenic mice. *J. Neurochem.* **79**, 1059–1064.

Tomita H., Shakkottai V. G., Gutman G. A., Sun G., Bunney W. E., Cahalan M. D., Chandy K. G. and Gargus J. J. (2003) Novel truncated isoform of SK3 potassium channel is a potent dominant-negative regulator of SK currents: implications in schizophrenia. *Mol. Psychiatry* **8**, 524–535.

Vesce S., Rossi D., Brambilla L. and Volterra A. (2007) Glutamate release from astrocytes in physiological conditions and in neuro-degenerative disorders characterized by neuroinflammation. *Int. Rev. Neurobiol.* **82**, 57–71.

Villalobos C., Shakkottai V. G., Chandy K. G., Michelhaugh S. K. and Andrade R. (2004) SKCa channels mediate the medium but not the slow calcium-activated afterhyperpolarization in cortical neurons. *J. Neurosci.* **24**, 3537–3542.

Viviani B., Gardoni F. and Marinovich M. (2007) Cytokines and neuronal ion channels in health and disease. *Int. Rev. Neurobiol.* **82**, 247–263.

